

INTERNATIONAL SOCIETY FOR SOIL MECHANICS AND GEOTECHNICAL ENGINEERING



This paper was downloaded from the Online Library of the International Society for Soil Mechanics and Geotechnical Engineering (ISSMGE). The library is available here:

<https://www.issmge.org/publications/online-library>

This is an open-access database that archives thousands of papers published under the Auspices of the ISSMGE and maintained by the Innovation and Development Committee of ISSMGE.

The paper was published in the proceedings of the 20th International Conference on Soil Mechanics and Geotechnical Engineering and was edited by Mizanur Rahman and Mark Jaksa. The conference was held from May 1st to May 5th 2022 in Sydney, Australia.

Innovative design of soil nail wall with the consideration of soil suction

Conception innovante d'un mur d'ongles de sol avec la considération de l'aspiration du sol

Bosco Poon

GHD Pty Ltd, NSW, Australia

Peter Mitchell

The University of Adelaide, SA, Australia

ABSTRACT: The effective stress concept for unsaturated soils has been applied to the design and construction of up to an 8.9m high retaining wall excavation as part of an expressway construction in Adelaide, South Australia. The geotechnical investigations indicated that the regional groundwater was well below the proposed excavation. The non-fissured clay encountered over the proposed excavation depth was unsaturated, with a lower bound soil suction value of pF 3.6 considered in the design. The shear strength of the unsaturated clay, quantified by soil suction, was significantly greater than that derived based on conventional saturated soil mechanics. This allowed the use of a lighter retaining structure with considerable cost savings. The adopted retention system for the excavation was soil nail with fiber shotcrete facing. One challenge to the design was the swelling behavior of the unsaturated clay when wetted from their original high soil suction condition. While the effect of swelling did not affect global slope stability, it affected the tensile force in the nails and the design of the nail-heads and shotcrete facing. The design principle adopted was to reduce load that the retaining system had to accommodate, by providing a flexible facing system that was permitted to deform within acceptable limits, while remaining serviceable for the long term wall deflection due to changes in soil suction after the completion of construction. This paper focuses on the geotechnical design aspect of the soil nail wall. Comparison between the design and measured wall movements is also presented.

RÉSUMÉ : Le concept de contrainte efficace sur les sols non saturés a été appliqué à la conception et à la construction d'une excavation de mur de soutènement jusqu'à 8,9 m de haut dans le cadre d'une construction d'autoroute à Adélaïde, en Australie-Méridionale. Les études géotechniques ont indiqué que les eaux souterraines régionales étaient bien en dessous de l'excavation proposée. L'argile non fissurée rencontrée sur la profondeur d'excavation proposée n'était pas saturée, avec une valeur limite inférieure d'aspiration du sol de pF 3,6 prise en compte dans la conception. La résistance au cisaillement de l'argile non saturée, quantifiée par la succion du sol, était significativement plus élevée que celle obtenue sur la base de la mécanique conventionnelle des sols saturés. Cela a permis l'utilisation d'une structure de retenue plus légère avec des économies de coûts considérables. Le système de rétention adopté pour l'excavation était un clou de sol avec revêtement en béton projeté en fibre. L'un des défis de la conception était le comportement au gonflement de l'argile non saturée lorsqu'elle était mouillée par rapport à son état d'origine de forte aspiration du sol. Bien que l'effet du gonflement n'affecte pas la stabilité globale de la pente, il a affecté la force de traction dans le clou et la conception de la tête de clou et du revêtement en béton projeté. Le principe de conception adopté était de réduire la charge que le système de retenue devait supporter, en fournissant un système de revêtement flexible qui était autorisé à se déformer dans des limites acceptables, tout en restant utilisable pour la flèche à long terme du mur en raison des changements d'aspiration du sol après l'achèvement de construction. Cet article se concentre sur l'aspect de conception géotechnique du mur de clou de sol. Une comparaison entre la conception et les mouvements de mur mesurés est également présentée.

KEYWORDS: Unsaturated soil mechanics, swelling pressure, soil nail wall, soil suction.

1 INTRODUCTION.

The concept of unsaturated soil mechanics was applied in soil nail wall design for an area with predominately stiff/very stiff clay above relatively deep groundwater table. The project was a 3.7 km long road upgrade between Torrens Road and the River Torrens located at about 5km northwest of Adelaide CBD. The road upgrade involved the construction of a 3km long lowered road section of up to 8.9m deep cutting with soil nail reinforcement. The project area has a deep Quaternary alluvial profile. The regional groundwater occurs in a gravelly aquifer at depths of about 9 to 14m beneath ground surface, which is reflective of the level in the River Torrens. The soil above the aquifer, where the lowered road is formed, is typically stiff to very stiff clays with sandy lenses. The clays are of low to medium plasticity. The soil profile beneath the aquifer is a deep deposition of predominately very stiff to hard clays. As the excavation depth is permanently above the water table, the design philosophy adopted for the soil nail walls considers that the clays are unsaturated in the long term and the shear strength is governed by soil suction effects. The geotechnical

investigations indicated that no significant soil defects (e.g. fissuring) were present in the clays. It was assumed that if such features exist, they were localised and of limited lateral extent.

This paper presents the design methodology of the soil nail walls in unsaturated expansive clay, including the selection of design soil suction and shear strength profile, the adoption of appropriate bond strength and the assessment of potential swelling pressure to inform soil nail and shotcrete designs. Comparison between the design and measured wall movements is also presented.

2 DESIGN SOIL SUCTION PROFILES

The total soil suction is a measure of the potential for the soil to undergo a change in moisture content and is related to the water vapour pressure in the air space of the soil. It can be measured by devices (such as psychrometers) capable of measuring relative humidity. The total suction of a soil consists of two components: matric suction and osmotic suction. The definitions for the two components have been described in unsaturated soil mechanics textbooks (e.g. Briaud 2013). The measurement of soil suction is

in units of kPa, or alternatively in logarithm of pore water potential, pF. The conversion from kPa to pF is given by:

$$\text{suction (kPa)} = 9.81 \times 10^{(pF-2)} \quad (1)$$

The soil suction profiles for the project site were investigated by the South Australian Department of Planning, Transport and Infrastructure (DPTI) through a soil wetting process in a piled wall trial located at Robert Street next to the project corridor. The in-situ total soil suction values were assessed from psychrometer tests on borehole samples obtained prior to the trial. The clays were in a relatively dry condition and the measured total suctions were up to about pF = 4.8 as shown in Figure 1.

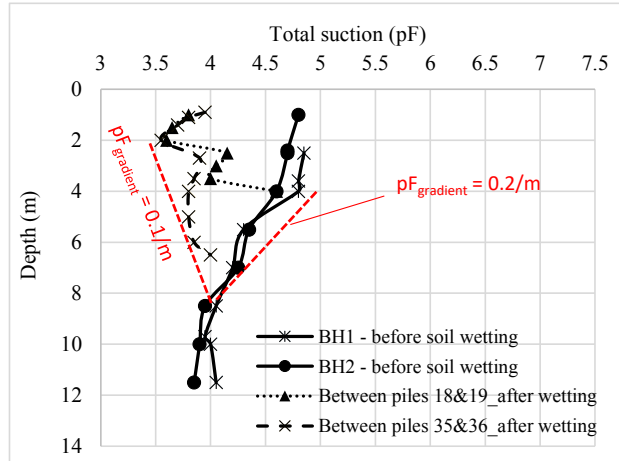


Figure 1. Total suction profiles

After the piled wall excavation to a depth of 8m, water was injected into a 1.5m deep soakage trench located at 1m away from the rear of the wall over a period of 3 to 4 weeks. The measured suction values after the soil wetting, as shown in Figure 1, was as low as about pF = 3.6. For design purposes, pF = 3.6 was considered representative for long-term wetted soil condition. pF = 3.4 was used for the adverse case of a prolonged leakage from a broken water pipe.

3 DESIGN SHEAR STRENGTH

The shear strength of unsaturated clay was assessed from the equation of Fredlund and Rahardjo (1993):

$$\tau_f = c' + \sigma'_v \tan \phi' + u_w \tan \phi^b \quad (2)$$

where τ_f = shear strength, c' = effective cohesion, ϕ' = effective friction angle, σ'_v = effective stress on failure plane, u_w = matric suction and $\tan \phi^b$ = rate of increase in shear strength with increase in matric suction. For practical design purposes, total suction (i.e. matric suction plus osmotic suction), rather than the matric suction, was used in Eq. 2. This is because the osmotic pressure was much less than the measured total suction, and the total and matric suction curves were almost congruent.

The effective strength parameters, c' and ϕ' , were assessed based on 33 CU triaxial test results. A linear regression line drawn to the p-q plot indicated that $c' = 9.5$ kPa and $\phi' = 30.7^\circ$. For design purposes, the characteristic strength values of $c' = 5$ kPa and $\phi' = 30^\circ$ were adopted.

To assess the appropriate value of ϕ^b and hence the suction induced strength, test data of Keswick clay in Adelaide by Richards (1977) and Woodburn (1997) was compiled and plotted in Figure 2. This figure indicates a linear relationship between shear strength and total suction. The mean value of the measured $\tan \phi^b$ is 0.15, and the upper and lower bound values were considered to be 0.22 and 0.11, respectively. For design

purposes, the mean $\tan \phi^b$ value of 0.15 was adopted and the corresponding ϕ^b value was 8.5° .

Figure 3 shows the plot of apparent cohesion vs total suction. In particular, the apparent cohesion given by Fredlund and Rahardjo (1993) was assessed based on the following particular terms from Eq.2

$$\text{Apparent cohesion} = c' + u_w \tan \phi^b \quad (3)$$

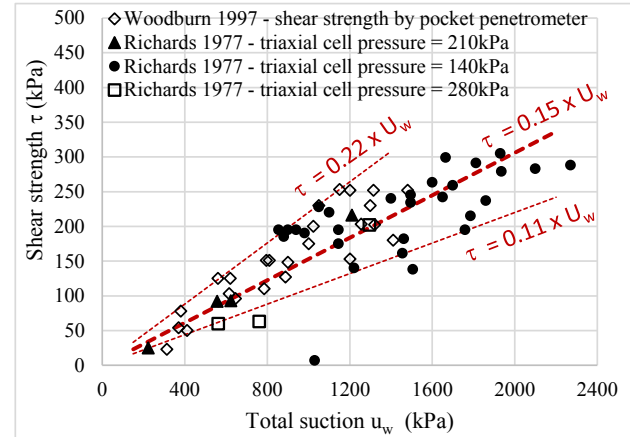


Figure 2. Shear strength vs. total suction

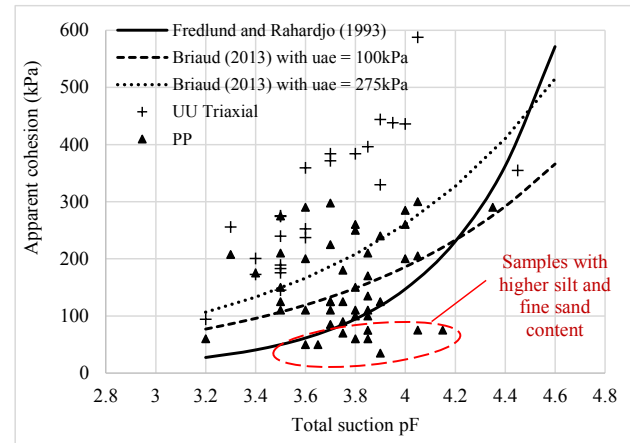


Figure 3. Apparent cohesion vs total suction

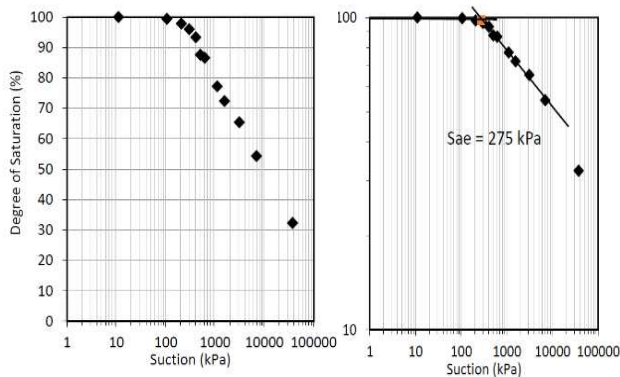
It can be seen that the assessed apparent cohesion values based on the Eq. 3 are much lower than the laboratory data where soil suction tests were conducted on tube samples that were also used in UU triaxial tests under the applied cell pressures of 40 – 200kPa. Conversely, pocket penetrometer (PP) tests on soil samples are not subject to overburden pressures and the results are closer to predictions. Note that some soil samples have higher silt and fine sand content, the bonds between the grains are weak and easily broken upon PP testing, leading to lower inferred shear strengths than predictions. Also shown on Figure 3 is the apparent cohesion estimated using Briaud (2013) in conjunction with the effective stress parameter χ given by Khalili and Khabbaz (1998):

$$\text{Apparent cohesion} = c' + \chi \cdot u_w \tan \phi',$$

$$\text{and} \quad \chi \cdot u_w = \sqrt{u_{ae} \cdot u_w} \quad (4)$$

where u_{ae} is the suction at air entry, which may be taken as 100kPa for Adelaide clays in general. Desa and Scott (2018) presented the project specific soil water characteristic curve (SWCC) of the tested clay samples obtained from the piled wall trial site. The measured air entry value was found to be approximately 275kPa as shown in Figure 4.

By considering both u_{ae} values of 100kPa and 275kPa, Figure 3 shows that the Briaud relationship gives a higher predicted apparent cohesion than that of Eq. 3 at a suction range below $pF = 4.2$. For design purposes, an apparent cohesion of 40kPa was adopted for long-term design calculated based on Fredlund and



Rahardjo (1993) (i.e. Eq.3) for a design total suction of $pF3.4$. This is deemed to be erring on the safe side as the assessed value is generally lower than those of UU triaxial and PP results, as well as that given by Briaud (2013), i.e., Eq. 4. Figure 4. Project specific SWCC drying curve in (a) semi-log scale and (b) log-log scale (Desa and Scott)

The stability of the soil nail walls has adopted strength parameters and minimum permissible design Factors of Safety (FoS) appropriate for the various load cases and soil conditions. This method is considered preferable to the use of partial factors (as suggested by AS4678) in unsaturated soils as the analyses are considered to be more transparent. The FoS against global failure presented in Table 1 have been adopted for the wall designs. These FoS are generally consistent with the intent outlined in CIRIA C580 in which moderately conservative, worst credible and most probable scenarios are considered.

Table 1. FoS adopted in design

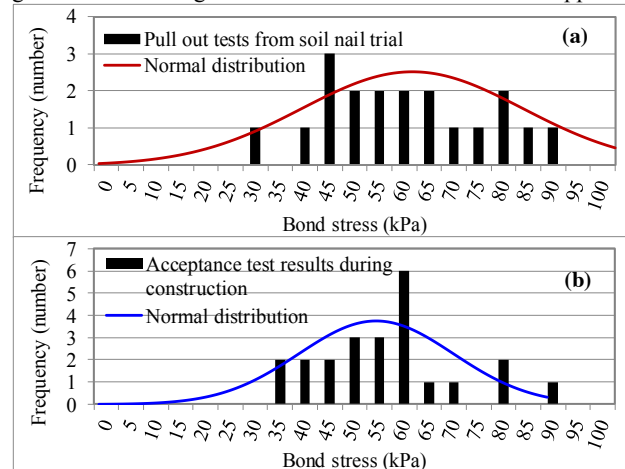
Wall Condition	Assumed Soil & Load Conditions	FoS (minimum)
Temporary – wedge failure mode ⁽¹⁾	Equilibrium soil suction ($pF=4.0$)	1.25
Temporary – global stability ⁽²⁾	Equilibrium soil suction ($pF=4.0$)	1.3
Permanent – global stability ⁽²⁾	Equilibrium soil suction ($pF=4.0$)	1.5
Permanent ⁽³⁾ – global stability	Long term wetted soil suction ($pF=3.4$)	1.35
Temporary – global ⁽¹⁾	Wetted + earthquake	1.05
Temporary – global ⁽¹⁾	Wetted + collision	1.05

(1) Worst credible; (2) Most probable; (3) Moderately conservative

4 SOIL NAIL BOND STRENGTH

DPTI conducted a soil nail trial to inform the design and ultimate soil nail bond strength prior to construction. Two trial sites located at Robert Street and Gawler Street were selected next to the project corridor. At the Robert Street site where the pile wall trial was conducted, soil nails were installed between the existing piles. At the Gawler Street site the soil nails were installed in the 1V:1H side slopes of a 4m deep excavation. The soils at both sites consisted of very stiff to hard clay/silty clay, with local softening due to controlled soil wetting. A total of 20 pull-out tests were conducted at the trial sites of up to 6m below ground surface. The soil nails used in the trial and later during the production were 25mm threaded steel bars with approved spacers for the support as they were installed with various grouted lengths in 150 or 200mm diameter boreholes that were drilled with rotary drill bit with air flush. Figure 5a shows the frequency histogram of the measured ultimate bond strength during the

trial. The mean bond strength value is about 60kPa, which is about 0.3-0.4 times the undrained shear strength S_u of the clay that was estimated to be in the order of 150 – 200kPa. For design purposes, a lower bond strength of 40kPa representing an acceptable 10% failure rate was adopted. This design value was used in stability assessment for short-term cases. For long-term design where the soil was assumed in wetted condition, a geotechnical strength reduction factor of 0.67 was applied,



giving a long-term bond stress of 26.7kPa. This is consistent with the lowest pull-out test result of 30kPa in very wet soil condition.

Figure 5. Pull out tests from (a) soil nail trial by DPTI; (b) construction

Figure 5b shows the frequency histogram of the measured bond strengths in the acceptance tests during construction. These results are similar to those of the trial, with a mean bond strength value of about 55kPa. However 10% of the test result were found to be below the design bond strength of 40kPa. The contributory factors for these 10% of soil nails not achieving the design load could be: (i) wetter than expected soil conditions, resulting in loss of soil suction; and (ii) potential remoulding of the soil along the bond zone or inadequately roughened borehole.

Higher ultimate bond strengths were expected for sandy soils, although these soils do not appear to have been tested in the soil nail pull-out trial. The design bond strength for the medium dense and dense sand and silty sand was adopted conservatively as being equal to $\sigma'_{vo} \times \tan 35^\circ$, where σ'_{vo} is the effective vertical overburden pressure. However, the collapse of soil nail boreholes in clean sand may lead to a lower bond strength. To overcome this construction difficulty, self-drilling nails were later used for wall excavation in sandy soils. In general, the self-drilling nails achieved a higher pull-out resistance than that of the standard installation method. This was demonstrated by the verification test results. Figure 6 shows an exposed self-drilling nail.

Figure 6. Self-drilling nail



5 SWELL PRESSURE BEHIND WALL

When the soil suction in an unsaturated clay is decreased, the resulting swell can be reduced by increasing the confining pressure. Oedometer measurements of the pressure-swelling

response from soil samples taken from the project site are shown in Figure 7. It can be seen that the pressure-swell is non-linear, and a small pressure is sufficient to suppress a significant amount of soil swell. For design purposes, however, the swell pressure P , and the suppressed swell ($Y-\delta$) can be approximated by a linear relationship:

$$P = k(Y - \delta) \quad (5)$$

where Y is the soil swell under zero pressure, δ is the soil swell, and k is the swell stiffness, which is commonly taken to be 1000kPa/m for Adelaide clays (e.g., see discussion in AS2870-2011 clause F2(c)).

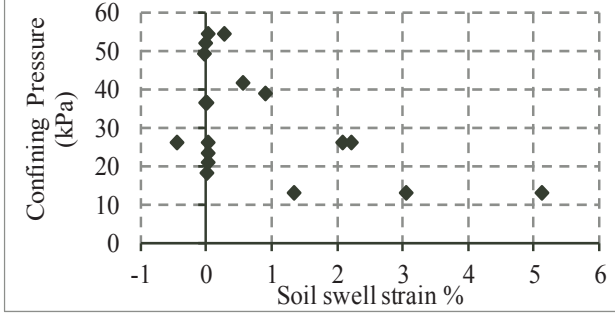


Figure 7. Pressure-swell measurements

For soil nail wall design, the effect of swelling does not affect global slope stability; it is an equal and opposite action that affects the tensile forces in the nail and the design of the nail head and shotcrete facing. Figure 8 shows the adopted nail pull-out analysis model, in which soil swelling within a swell zone width T , has resulted in a wall swell pressure W_p . The adopted rate of suction change $pF_{gradient}$, within the swelling zone varies from 0.1/m to 0.2/m, which reflects the worst case of pF gradient found in the suction profile shown in Figure 1. The adopted $pF_{gradient}$ range is conservative considering that the excavated face is sealed with shotcrete facing; the top of wall is covered by concrete barrier; and adequate drainage including strip drains and weep holes are in place.

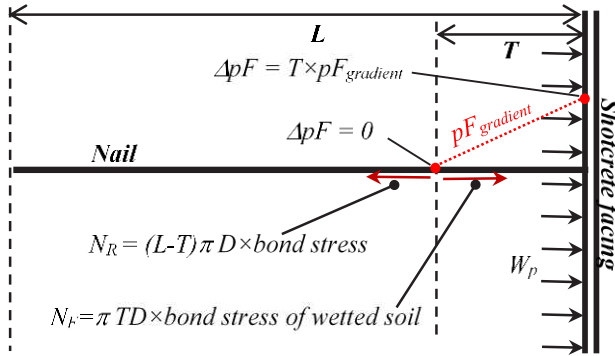


Figure 8. Nail pull-out analysis model

The average suction change, $\Delta pF_{average}$, within the swelling zone can be calculated by:

$$\Delta pF_{average} = [T \times pF_{gradient}] / 2 \quad (6)$$

The free swell, Y , corresponding to the adopted $\Delta pF_{average}$ within the swell zone width T is given by:

$$Y = T \times \Delta pF_{average} \times I_{pt} \quad (7)$$

where I_{pt} is the Instability Index, measured to be about 1%. Substituting Eqs. (6) and (7) into (5) gives:

$$W_p = k(T^2 \times pF_{gradient} \times I_{pt} / 2 - \delta_{wall}) \quad (8)$$

A series of finite element analyses (FEA) using SIGMA/W was carried out to simulate the soil nail walls under swell conditions. The analysis results indicated that soil nail walls of different wall heights and soil nail configurations deflect typically 3mm when 10kPa swelling pressure was applied behind the walls (see Figure 9). The wall deflections δ_{wall} for other swelling pressures in the neighborhood of 10kPa (say 0-20kPa) can be proportioned against this FEA result:

$$\delta_{wall} = W_p \times 0.003[m] / 10[kPa] \quad (9)$$

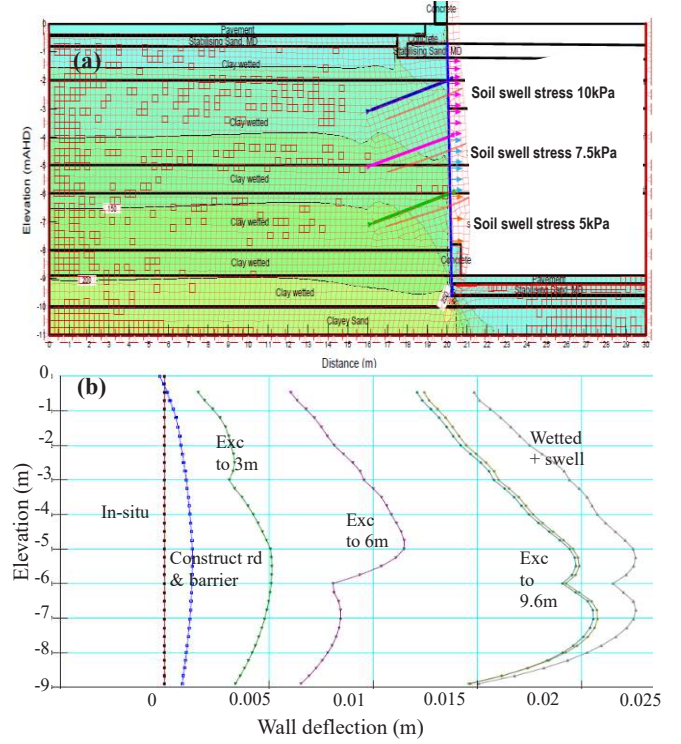


Figure 9. (a) FEA geometry, (b) Predicted wall deflection with imposed 10kPa swelling pressure behind the wall face for different excavation

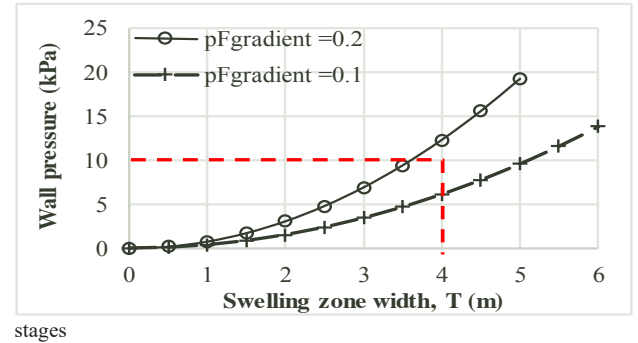


Figure 10. Assessed wall pressure vs. swelling zone

Combining Eqs. (8) and (9) and applying $k = 1000\text{kPa/m}$ and $I_{pt} = 0.01$ (i.e. 1%) gives:

$$W_p = 3.85 \times T^2 \times pF_{gradient} \quad (10)$$

Figure 10 shows the plot of W_p vs T based on Eq. (10). CPT soundings taken after wetting of the Robert Street trial piled wall site indicated a horizontal extent of wetting of typically 2-3m from the back of the wall face, and no more than 4m. Therefore, Figure 10 demonstrates that the swell pressures generated are almost always within 10kPa for $T < 4\text{m}$. With the W_p assessed, the nail resisting force N_R to resist the nail swelling force, N_F , and the wall swelling load, W_F , are given by:

$$N_R = N_F + W_F \quad (11)$$

$$N_R = (L - T) \times \pi \times D \times \text{bond stress} \quad (12)$$

$$N_F = \pi D \times T \times \text{bond stress of wetted soil (26.7kPa)} \quad (13)$$

$$W_F = W_p \times \text{soil nail tributary area} \quad (14)$$

The face of the soil nailed walls was lined with typically 75mm thick synthetic fiber reinforced shotcrete (Figure 11) but was locally thickened over nail heads and at certain mid-span locations where required. The shotcrete was designed to resist the lateral pressures associated with clay swelling and sand lenses, as well as to resist the punching effect at the nail head.



Figure 11. Assessed wall pressure vs. swelling zone

6 SOIL NAIL WALL DESIGN CONFIGURATIONS

The soil nail walls vary in height up to a maximum of about 8.9m. It was constructed with a subvertical slope face no steeper than 1H:40V and covered with a 75mm (typical) thick synthetic fiber reinforced shotcrete facing. The drilled holes for the soil nails are inclined at an angle of 15 degrees to the horizontal and are 150mm in diameter, but increased to 200mm diameter in sandy soil and softened clay areas with remoulding issues of the clay soil along the bond zone. The design of the soil nail wall has taken into consideration the global failure mode as well as a nominally 1m wide local wedge failure surface as shown in Figure 12a. Up to five rows of soil nails are adopted, depending on the wall height, proximity to services, and ground condition encountered.

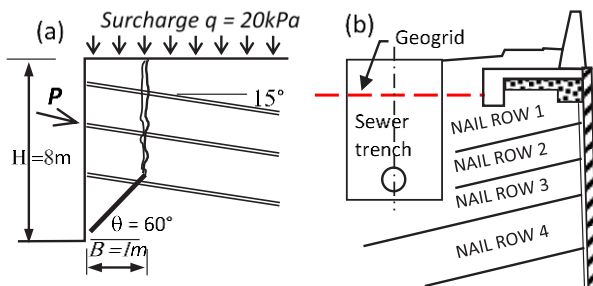


Figure 12. (a) Wedge failure mechanism (b) Design of soil nail wall near existing sewer trench

For an 8 m high wall excavation in unsaturated clay, three rows of 4.5 to 6m long soil nails were required (see Figure 12a). The vertical and horizontal spacing between nails were 2.5m and 3m, respectively. For clay profile with interbedded sand lenses, the nail lengths were increased to 5 – 7m and the nail spacing reduced to 1.5m vertically and 2.1m horizontally. The proximity of sewer trench had a marked impact on the global stability, particularly as the upper nail lengths were limited to before the trench in case unforeseen emergency repairs are required. To achieve a satisfactory FoS for wall stability, a layer of geogrid was installed over the trench at the underside of the pavement (Figure 12b). This is to provide extra tensile reinforcement and alter the failure surface geometry.

7 CONSTRUCTION METHOD

An observational method (Figure 13) was adopted for soil nail wall construction, whereby a temporary bench was created in front of each excavation lift, so a visual assessment of the ground conditions could be made. This allowed time for the geotechnical site representative to confirm the ground conditions and to select suitable soil nail arrangements from the toolbox designs that were pre-developed during the detailed design stage for a range of possible soil profiles and unfavorable ground conditions (such as sand lenses, unsaturated fissured clay and perched groundwater). Upon final trim of the temporary bench for each excavation lift, the ground conditions were re-inspected prior to installation of soil nail and shotcrete.

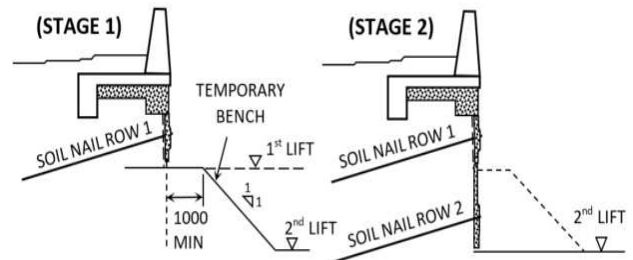


Figure 13. Assessed wall pressure vs. swelling zone

8 WALL MOVEMENTS

Monitoring of the soil nail walls was carried out during construction and over the service life using a system of inclinometers and survey markers. For wall excavation in the clayey soil profile (typically stiff to very stiff consistency), the registered wall deflection during construction was small. As shown in Figure 14, the maximum deflection was typically less than 0.25% of the excavation depth in clay.

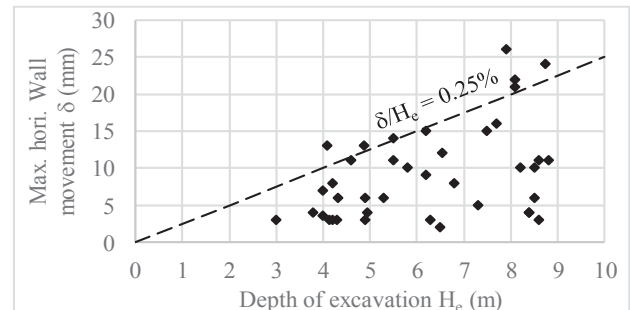


Figure 14. Assessed wall pressure vs. swelling zone

Sand lenses (some pockets of cohesionless sand and silty sand) of varying thicknesses and of varying depths were encountered in the southern part of the wall alignment. The occurrence of sand lenses at the base or mid-height of a cut was deemed to be more critical to global stability than a sand lens near the top of the wall. Figure 15 shows an over break that occurred during excavation of a wall section in a moderately thick, clean sand layer encountered at depth of 3.3 to 5.1m below top of the wall. The total retaining height at this wall section was 8m and was constructed in staged excavation. After the completion of the 2nd lift excavation to a depth of 5.3m below wall top, the exposed cut face was not covered with shotcrete immediately due to unexpected construction delays. As the exposed face lost moisture, this led to a significant unravelling of the sandy soil and resulted in soil caving-in, with a typical undercut size of 0.5m wide by 1.3m high. Wall movements exceeding design predictions were observed, with a horizontal and vertical displacement of up to 25mm and 14mm, respectively, being measured at the top of wall. Longitudinal

cracks of up to 7mm wide were observed at the pavement behind the wall. The cracks were formed parallel with the road alignment at an offset distance of 2 to 2.5m from the inner side of the crash barrier, which coincided with the footing heel of the barrier. Coring investigations along the length of the cracks indicated that they were generally terminated at the bottom of the base course of the pavement structure, about 650mm below pavement surface. Notwithstanding the surface cracks outlined, the wall top deflection was at 0.47% of the excavated depth, which was still within 0.2 to 0.5% range commonly observed for wall excavation in stiff clays.

Figure 15. Site photo on the cave-in of the exposed sand layer

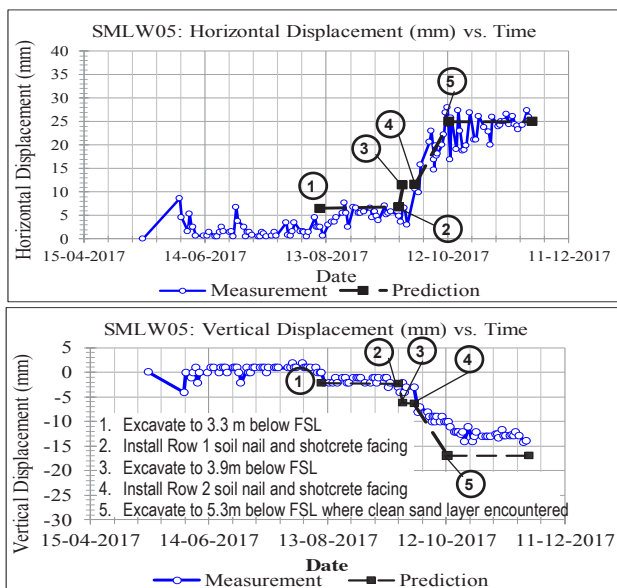


Figure 16. Back-analysed wall movements vs. measurements

In light of the wall movements, back analysis based on 2D FEA using the PLAXIS 2D was carried out. The back-analysis results matched successfully with the measured top of wall displacement as shown in Figure 16. The volumetric strain plot (Figure 17) obtained from FEA exhibits similar features to those of observation including: (i) a potential wedge failure at the exposed cut face; and (ii) a shallow crack zone behind the footing heel of the crash barrier. The global stability of the wall was also assessed in FEA using the c' - ϕ' reduction approach, and supplemented by conventional limit equilibrium approach using Morgenstern Price method of slices. Both analysis results indicated that while the FoS is satisfactory for short term excavation to mid-height of the wall, the formation of tension cracks has resulted in a lower FoS than 1.35 after full depth excavation and under long-term wetted soil suction condition ($pF=3.4$). For the remedial design using extra soil nails, a 1m wide tension crack zone at 2m depth was considered behind the footing heel of the crash barrier. Figure 11 shows the finished wall after full depth excavation.

9 CONCLUSION

The relative deep groundwater level and predominately unsaturated and non-fissured clay ground conditions were ideal for wall design using unsaturated soil mechanics. This allowed the use of a lighter retaining structure with considerable cost savings. The wall excavation was reinforced by soil nails and a typically 75mm thick fiber shotcrete facing. One challenge to the design is the effect of swelling on lateral stress and deformation in soil. While soil swelling does not affect global slope stability, it affects the tensile force in the nail and the design of the nail-head and shotcrete facing. It has been demonstrated that the swell pressure generated due to the suction change is less than 10kPa.

The subject soil nail wall in the unsaturated clay was not immune to construction issues. The excavation through some of the thick and clean sand lenses within the clay profile caused significant over-break, leading to greater wall movements than anticipated. An observational approach was implemented to cope with the soil variability and to reduce the risks of over-break. This required the presence of geotechnical site representatives to inspect the exposed face and select a suitable soil nail arrangement from the design toolbox (predefined designs for a range of possible soil profiles).

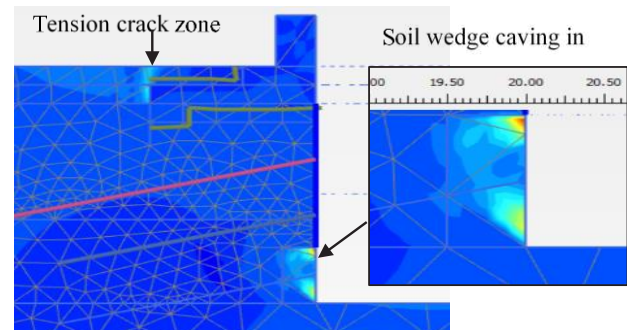


Figure 17. Potential tension crack and cave-in from FEA

10 ACKNOWLEDGEMENTS

The authors acknowledge the work of many others, including Aurecon, the Department of Planning, Transport and Infrastructure (DPTI), CPB Contractors, York Civil, Mott MacDonald, WGA, and Mr Richard Herraman formerly of DPTI, that made the project a success

11 REFERENCES

- AS2870-2011 Residential slabs and footings. Standards Aust.
- AS4678-2002 Earth Retaining Structures. Standards Australia.
- Briaud J-L., (2013) Geotechnical engineering: Unsaturated and saturated soils. John Wiley & Sons.
- Desa, S.A.J., Scott, B.T. (2018). Inferring soil water characteristics for Adelaide clay using fractal theory. Australian Geomechanics J., Vol. 53, No.1, pp.127 – 135.
- Fredlund, D. G., Rahardjo, H. (1993). Soil Mechanics for Unsaturated Soils. John Wiley & Sons.
- Gaba A.R., Simpson B., Powrie W., and Beadman D.R. (2003). Embedded retaining walls – guidance for economic design. CIRIA Report C580, London: CIRIA 390pp.
- Khalili, N., Khabbaz, M.H. (1998). A unique relationship for χ for the determination of the shear strength of unsaturated soils. Geotechnique. 39(5): 681-687.
- Richards, B.G. (1977), Pressures on a Retaining Wall by an Expansive Clay. Proc. 9th ICSMFE, 2/72, pp. 705-710, Tokyo.
- Woodburn, J. A. (1997) Report No GSU 1061 for the Department of Planning, Transport and Infrastructure of SA.